

Ambient-Pressure Organic Superconductors κ -(DMEDO-TSeF)₂[Au(CN)₄](solv.): T_c Tuning by Modification of the Solvent of Crystallization**

Takashi Shirahata,^[a, b] Megumi Kibune,^[a] Hiroko Yoshino,^[a] and Tatsuro Imakubo*^[a]

Abstract: The unsymmetrical π donor dimethyl(ethylenedioxy)tetraselenafulvalene (DMEDO-TSeF) has provided six new organic superconductors with a monovalent square-planar [Au(CN)₄]⁻ ion and cyclic ethers as solvent of crystallization. The six new organic superconductors κ -(DMEDO-TSeF)₂[Au(CN)₄](solv.) [solv. = 1,3-dioxolane (DOL), 2,5-dihydrofuran (DHF), tetrahydropyran (THP), 1,3-dioxane (1,3-DOX), 3,4-dihydro-2H-pyran (DHP), or 1,4-dioxane (1,4-DOX)] are classified into two subphases κ_L and κ' according to the differ-

ences in their space group symmetry. κ_L -(DMEDO-TSeF)₂[Au(CN)₄](solv.) (solv. = DOL, DHF, THP, 1,3-DOX or DHP) crystallizes in the orthorhombic space group *Pnma*, and T_c of the κ_L phase varies by 1.7–5.3 K according to the size and shape of the solvent of crystallization. On the other hand, κ' -(DMEDO-TSeF)₂[Au(CN)₄](solv.) (solv. = DOL or 1,4-DOX) crystallizes

in the noncentrosymmetric monoclinic space group *Cc*. The κ' -phase containing 1,4-DOX shows superconductivity at 4.2 K, but the κ' -phase containing DOL does not show superconductivity down to 1.4 K. Systematic investigation of the six new organic superconductors, together with the two previously reported superconductors κ_H - and κ_L -(DMEDO-TSeF)₂[Au(CN)₄](THF), revealed that the T_c of the present system is finely tunable by utilizing the effect of the solvent of crystallization.

Keywords: fulvalenes • hydrogen bonds • solvent effects • superconductors • supramolecular chemistry

Introduction

Among the large number of substituents on organic π donors based on tetrathiafulvalene (TTF), the ethylenedioxy group gives characteristic features such as high solubility in common organic solvents and the ability to construct CH...O hydrogen bonds.^[1] The symmetrical derivative bis(ethylenedioxy)tetrathiafulvalene (BEDO-TTF or BO)^[2] has provided various organic metals containing two organic superconductors,^[3] and a giant photoresponse has been report-

ed for the PF₆⁻ salt of ethylenedioxytetrathiafulvalene (EDO-TTF), which is a hybrid of BO and pristine TTF.^[4] In spite of these successful results on TTF derivatives, there are few reports on tetraselenafulvalene (TSeF) derivatives bearing a ethylenedioxy group because of difficulties in synthesis. Recently, we reported the safe synthesis of bis(ethylenedioxy)tetraselenafulvalene (BEDO-TSeF)^[5] and dimethyl(ethylenedioxy)tetraselenafulvalene (DMEDO-TSeF)^[6] as promising π donors containing the ethylenedioxy group for the development of organic metals and superconductors without the use of highly hazardous CSe₂. The latter molecule DMEDO-TSeF is the hybrid of tetramethyltetraselenafulvalene (TMTSF)^[7] and BEDO-TSeF, and it is also the chalcogen analogue of dimethyl(ethylenedithio)diselenadithiafulvalene (DMET), which provided the first organic superconductor based on an unsymmetrical organic π donor.^[8] We began research on the cation radical salts of DMEDO-TSeF with the octahedral anions PF₆⁻, AsF₆⁻, and SbF₆⁻.^[9] The donor packing motifs (so-called β -type) and quasi-one-dimensional electronic band structures of these three salts are similar to those of the first organic superconductor (TMTSF)₂PF₆,^[9] but unfortunately no sign of superconductivity was observed. In the search for new organic supercon-

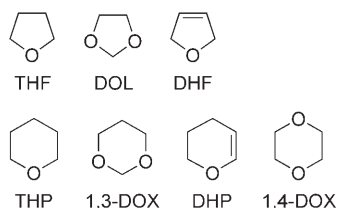
[a] Dr. T. Shirahata, M. Kibune, H. Yoshino, Dr. T. Imakubo
Imakubo Initiative Research Unit, RIKEN
2-1 Hirosawa, Wako, Saitama 351-0198 (Japan)
Fax: (+81)48-467-8790
E-mail: imakubo@riken.jp

[b] Dr. T. Shirahata
Current address:
Department of Chemistry and Materials Science
Tokyo Institute of Technology
O-okayama, Tokyo 152-8552 (Japan)

[**] DMEDO-TSeF = dimethyl(ethylenedioxy)tetraselenafulvalene.

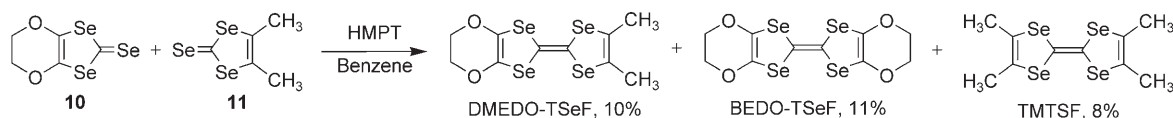
Supporting information for this article is available on the WWW under <http://www.chemurj.org/> or from the author.

ductors based on DMEDO-TSeF, we have tried counter anions with a variety of sizes and shapes and focused on monovalent square-planar organometallic anions, which have provided unique organic superconductors such as θ -(DIETS)₂[Au(CN)₄] (DIETS = diiodo(ethylenedithio)diselenadithiafulvalene)^[10] and κ -(BEDT-TTF)₂[M(CF₃)₄](1,1,2-trichloroethane) (BEDT-TTF = bis(ethylenedithio)tetrathiafulvalene; M = Cu, Ag, and Au).^[11] The former shows superconductivity under uniaxial strain applied along the I \cdots N bond, and the latter form two superconducting subphases (κ_H and κ_L), whereby the insulating layer in the κ_L -phase is much thicker than those of common organic superconductors. Inspired by these successful results, we introduced the [Au(CN)₄]⁻ ion into the DMEDO-TSeF system and reported two new ambient-pressure organic superconductors: κ_H - and κ_L -(DMEDO-TSeF)₂[Au(CN)₄](THF) (**1**: κ_H -phase; **2**: κ_L -phase).^[12] Twenty-five years after TMTSF, DMEDO-TSeF is the second example of a sulfur-free donor providing a bulk organic superconductor.^[13] It is well-known that T_c of an organic superconductor is sensitive to small structural changes in counter anions and/or solvent of crystallization,^[11,14] and from this point of view the above two DMEDO-TSeF-based organic superconductors seem to be suitable candidates for T_c tuning by modification of the solvent of crystallization. Furthermore, the high solubility of DMEDO-TSeF in common organic solvents is also advantageous for preparing the cation radical salts. Here we report on the synthesis, crystal structures, and physical properties of a series of cation radical salts κ_L -(DMEDO-TSeF)₂[Au(CN)₄](solv.) [solv. = 1,3-dioxolane (DOL) (**3**), 2,5-dihydrofuran (DHF) (**4**), tetrahydropyran (THP) (**5**), 1,3-dioxane (1,3-DOX) (**6**), or 3,4-dihydro-2H-pyran (DHP) (**7**)] and κ' -(DMEDO-TSeF)₂[Au(CN)₄](solv.) [solv. = DOL (**8**) or 1,4-dioxane (1,4-DOX) (**9**)] including six new ambient-pressure organic superconductors, comparison with the parent superconductors **1** and **2**, and experimental details of the synthesis of DMEDO-TSeF.



Results and Discussion

Donor synthesis: Neutral DMEDO-TSeF was synthesized by cross-coupling of the corresponding 1,3-diselenole-2-selenones **10** and **11** according to the literature,^[6] (Scheme 1)



Scheme 1. Synthesis of DMEDO-TSeF.

and single crystals of neutral DMEDO-TSeF were grown by slow evaporation of a CS₂/*n*-hexane solution at room temperature. X-ray structure analysis was performed at 293^[6] and 150 K, and crystal data are summarized in Table 1. As

Table 1. Crystal data for neutral DMEDO-TSeF.

<i>T</i> [K]	293 ^[a]	150
formula	C ₁₀ H ₁₀ O ₂ Se ₄	C ₁₀ H ₁₀ O ₂ Se ₄
formula weight	478.02	478.02
crystal system	monoclinic	monoclinic
space group	<i>P</i> 2 ₁ / <i>c</i> (no. 14)	<i>P</i> 2 ₁ / <i>c</i> (no. 14)
<i>a</i> [Å]	13.930(4)	13.868(3)
<i>b</i> [Å]	8.267(2)	8.3621(16)
<i>c</i> [Å]	11.842(3)	11.462(2)
β [°]	109.470(6)	110.379(4)
<i>V</i> [Å ³]	1285.8(6)	1246.0(4)
<i>Z</i>	4	4
ρ_{calc} [g cm ⁻³]	2.469	2.548
μ [mm ⁻¹]	11.394	11.758
independent reflections	3228	3088
observed reflections [<i>I</i> > 2 σ (<i>I</i>)]	2210	2617
variable parameters	154	147
<i>R</i> _{int}	0.0502	0.0331
GOF	1.040	1.054
<i>R</i> 1, <i>wR</i> 2 [<i>I</i> > 2 σ (<i>I</i>)]	0.0460, 0.1057	0.0315, 0.0916
<i>R</i> 1, <i>wR</i> 2 (all data)	0.0753, 0.1173	0.0391, 0.0956

[a] Reflection data for reference^[6] were reanalyzed and the disorder model for the ethylene bridge was improved.

shown in Figure 1, the 4,5-dimethyl-1,3-diselenole unit derived from TMTSF is almost planar except for the hydrogen atoms of the methyl groups. On the other hand, the 1,3-diselenole ring of the 4,5-ethylenedioxy-1,3-diselenole unit derived from BEDO-TSeF is bent, and the folding angle increases at low temperature, from 18.9° at 293 K to 20.2° at 150 K. The disorder of the ethylene bridge observed at room temperature has disappeared at 150 K. DMEDO-TSeF shows two reversible redox waves, and the electrochemical properties of DMEDO-TSeF lie midway between those of the parent molecules TMTSF and BEDO-TSeF.^[6]

Preparation of cation-radical salts: Single crystals of the [Au(CN)₄]⁻ salts of DMEDO-TSeF were prepared by galvanostatic oxidation of a solution of the corresponding cyclic ether (DOL, DHF, THP, 1,3-DOX, DHP, or 1,4-DOX) containing DMEDO-TSeF and tetrabutylammonium tetracyanoaurate as supporting electrolyte. These new salts crystallize in the so-called κ -type structure and are classified into κ_L - and κ' -subphases according to their space-group symmetry. Electrochemical crystallization in DOL afforded two phases κ_L - and κ' -(DMEDO-TSeF)₂[Au(CN)₄](DOL) (**3**: κ_L -phase; **8**: κ' -phase). Salt **3** is isostructural with κ_L -phase salt **2**,^[12] whereas salt **8** crystallizes in the monoclinic *Cc* space

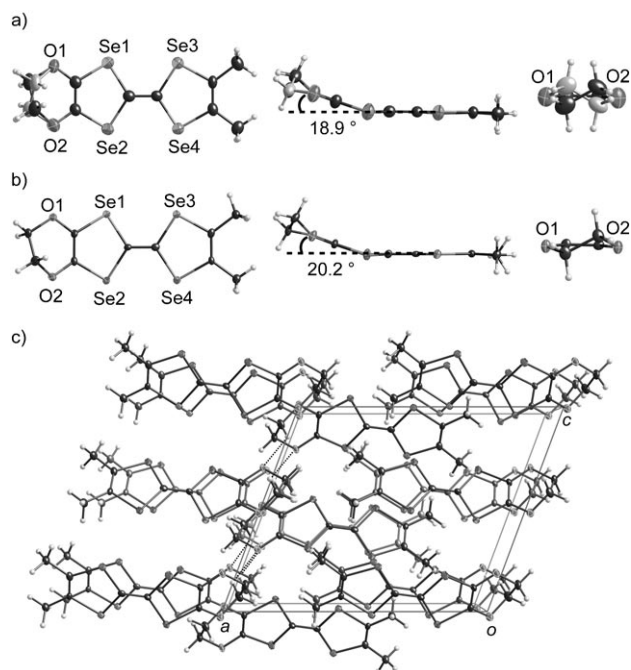


Figure 1. Molecular structures for DMEDO-TSeF at a) 293 K and b) 150 K: Top view (left), side view (center) and conformation of the ethylene group (right). Gray atoms and bonds represent minor orientation of the disordered ethylene bridge. c) Molecular packing motif at 150 K viewed along the crystallographic *b* axis. Dotted lines indicate CH...O contacts shorter than 2.72 Å.^[15]

group. Salts **3** and **8** cannot be distinguished by their crystal shape but can be identified by X-ray diffraction analysis, as in the case of salts **1** (κ_{H} -phase) and **2** (κ_{L} -phase), which simultaneously grow from THF solution.^[12] On the other hand, the cation radical salts containing DHP (**4**), THP (**5**),

1,3-DOX (**6**), DHP (**7**), or 1,4-DOX (**9**) crystallize in a single phase. Salts **4–7** belong to the κ_{L} -phase, and salt **9** belongs to the κ' -phase.

κ_{L} -(DMEDO-TSeF)₂[Au(CN)₄](solv.): X-ray structure analyses for the five new cation-radical salts of the κ_{L} -phase containing DOL (**3**), DHF (**4**), THP (**5**), 1,3-DOX (**6**), or DHP (**7**) as solvent of crystallization were performed at 293 and 150 K. They are isostructural with **2**^[12] and crystallize in the orthorhombic space group *Pnma* (Tables 2 and 3). The donor/anion/solvent ratios of these five salts are 2:1:1; the ratios and the nature of the solvent of crystallization were confirmed by elemental analyses and ¹H NMR spectroscopy, respectively. The molecular packing motif of **6** at 293 K is shown in Figure 2 as a representative of the κ_{L} -phase salts. The crystallographically equivalent Layers A and A' are separated by thick insulating layers (ca. 4.5–5.0 Å at 293 K, see Tables 2 and 3) composed of [Au(CN)₄][−] anions and solvent of crystallization.^[16] Many CH...N hydrogen bonds shorter than 2.75 Å^[15] exist between the donor molecule and the [Au(CN)₄][−] anion. The ethylene bridges of the donor molecules in **5**, **6**, and **7** show ordered conformations at 293 K, in contrast to those of **3** and **4**, which are disordered due to flipping, as well as **2** (Figure 3). Fractions of the major orientation increase to 80(2)% for **3** and 82(2)% for **4** at 150 K, but the disorder still persists (Table 4). Differences in the conformations of the ethylene bridges are related to the size of the solvent of crystallization, that is, salts **2–4** contain five-membered cyclic molecules, and salts **5–7** contain six-membered cyclic molecules. The smaller solvent of crystallization gives more clearance around the boundary of the layers and makes it easier for the ethylene bridges of the donor molecules to flip.

Table 2. Crystal data and transition temperature T_{c} (onset) for κ_{L} -phases **2–4**.

Compound (solv.)	2 (THF) ^[a]	3 (DOL)	4 (DHF)
<i>T</i> [K]	293	293	150
formula	C ₂₈ H ₂₈ AuN ₄ O ₅ Se ₈	C ₂₇ H ₂₆ AuN ₄ O ₆ Se ₈	C ₂₇ H ₂₆ AuN ₄ O ₆ Se ₈
formula weight	1329.19	1331.16	1331.16
crystal system	orthorhombic	orthorhombic	orthorhombic
space group	<i>Pnma</i> (no. 62)	<i>Pnma</i> (no. 62)	<i>Pnma</i> (no. 62)
<i>a</i> [Å]	8.3269(13)	8.2783(13)	8.2253(17)
<i>b</i> [Å]	38.638(6)	38.465(6)	38.307(8)
<i>c</i> [Å]	11.1203(17)	11.0850(16)	10.926(2)
<i>V</i> [Å ³]	3577.8(9)	3529.7(9)	3442.6(12)
<i>Z</i>	4	4	4
ρ_{calcd} [g cm ^{−3}]	2.468	2.505	2.568
μ [mm ^{−1}]	12.294	12.463	12.779
independent reflections	4572	4489	4406
observed reflections [<i>I</i> > 2 σ (<i>I</i>)]	2877	2916	3499
variable parameters	275	275	220
<i>R</i> _{int}	0.1050	0.1061	0.1002
GOF	0.967	0.966	1.175
<i>R</i> 1, <i>wR</i> 2 [<i>I</i> > 2 σ (<i>I</i>)]	0.0492, 0.1273	0.0426, 0.1082	0.0511, 0.1267
<i>R</i> 1, <i>wR</i> 2 (all data)	0.0806, 0.1369	0.0708, 0.1229	0.0664, 0.1377
thickness of insulating layer [Å]	4.9	4.5	4.3
<i>T</i> _c [K]	3.0		1.7
			4.2

[a] From reference [12].

Table 3. Crystal data and transition temperature T_c (onset) for κ_L -phases 5–7.

Compound (solv.)	5 (THP)		6 (1,3-DOX)		7 (DHP)	
T [K]	293	150	293	150	293	150
formula	$C_{29}H_{30}AuN_4O_5Se_8$	$C_{29}H_{30}AuN_4O_5Se_8$	$C_{28}H_{28}AuN_4O_6Se_8$	$C_{28}H_{28}AuN_4O_6Se_8$	$C_{29}H_{28}AuN_4O_5Se_8$	$C_{29}H_{28}AuN_4O_5Se_8$
formula weight	1343.22	1343.22	1345.19	1345.19	1341.20	1341.20
crystal system	orthorhombic	orthorhombic	orthorhombic	orthorhombic	orthorhombic	orthorhombic
space group	$Pnma$ (no. 62)					
a [Å]	8.3630(11)	8.2714(13)	8.3693(11)	8.3224(12)	8.3980(12)	8.3442(13)
b [Å]	38.892(5)	38.714(6)	38.799(5)	38.607(6)	39.000(5)	38.825(6)
c [Å]	11.2433(15)	11.0576(18)	11.0377(15)	10.8655(16)	11.0472(16)	10.8534(17)
V [Å ³]	3656.9(8)	3540.8(10)	3584.2(8)	3491.1(9)	3618.2(9)	3516.1(9)
Z	4	4	4	4	4	4
ρ_{calc} [g cm ⁻³]	2.440	2.520	2.493	2.559	2.462	2.534
μ [mm ⁻¹]	12.029	12.423	12.275	12.603	12.158	12.511
independent reflections	4610	4462	4597	4454	4663	4520
observed reflections [$I > 2\sigma(I)$]	2620	3553	2882	3569	2847	3359
variable parameters	237	237	219	219	237	237
R_{int}	0.1574	0.0923	0.1198	0.0910	0.1031	0.1260
GOF	0.884	1.150	0.932	1.029	0.948	1.122
$R1, wR2$ [$I > 2\sigma(I)$]	0.0602, 0.1461	0.0952, 0.2505	0.0450, 0.1071	0.0396, 0.0962	0.0477, 0.1196	0.0629, 0.1631
$R1, wR2$ (all data)	0.1015, 0.1574	0.1110, 0.2578	0.0802, 0.1148	0.0532, 0.0997	0.0811, 0.1270	0.0867, 0.1751
thickness of insulating layer [Å]	4.9	4.8	4.9	4.7	5.0	4.8
T_c [K]		4.5		2.6		5.3

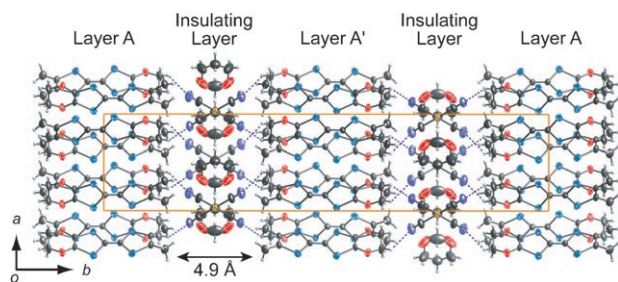


Figure 2. Molecular packing motif for **6** at 293 K. Dotted lines indicate $CH \cdots N$ contacts shorter than 2.75 Å.

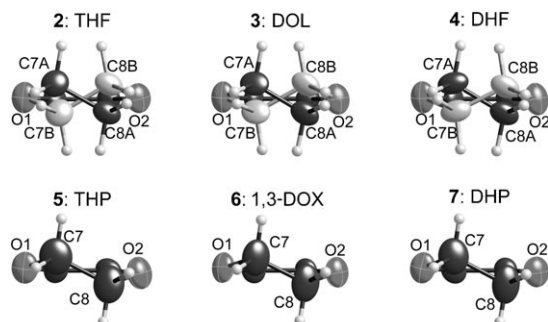


Figure 3. Conformations of the ethylenedioxy group of DMEDO-TSeF for **2–7** at 293 K. Gray atoms and bonds in **2–4** represent the minor orientations of the disordered ethylene bridge.

Table 4. Distributions of two orientations of disordered ethylene bridges.

Compound (solv.)	T [K]	Major [%]	Minor [%]
2 (THF) ^[a]	293	74(2)	26(2)
3 (DOL)	293	69(2)	31(2)
	150	80(2)	20(2)
4 (DHF)	293	70(2)	30(2)
	150	82(2)	18(2)

[a] From reference [12].

Figure 4a shows molecular arrangements of the conducting donor layer for **3** as a representative of the κ_L -phase salts. The head-to-tail dimers are arranged orthogonally, and

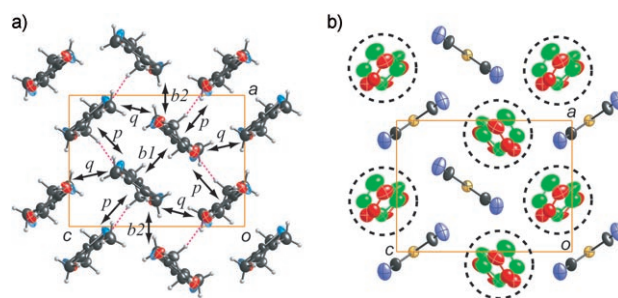


Figure 4. a) Donor arrangement of **3** at 293 K viewed along the crystallographic b axis. Dotted lines indicate $CH \cdots O$ contacts shorter than 2.72 Å. The minor orientations of the disordered ethylene bridge of the donor molecule are omitted for clarity. b) Crystal structure of the insulating layer for **3** at 293 K projected onto the ac plane. Red and green indicate configurations A and B of the disordered DOL molecules, respectively (positions generated by the mirror symmetry operation are omitted for clarity).

the donor arrangement within the donor layer is of the so-called κ -type. The $CH \cdots O$ hydrogen bonds are constructed along the interaction p and run along the a axis. The solvent of crystallization is located in cavities formed by the herringbone-type arrangement of anions (Figure 4b). The molecular arrangements of the donor layer for the other κ_L -phase salts are the same as that of **3**, but there are marked differences in the configuration of the solvent of crystallization among the κ_L -phase salts. In salt **3**, configurations A (60%) and B (40%) of the DOL molecule, which are represented by red and green in Figure 4b, are located in the general position around the mirror plane. Therefore, extreme disorder

due to the $2 \times 2 = 4$ conformations is observed at 293 K (Figure 5, top left), as well as for the THF molecules in **2**.^[12] Similar complicated disorder of the solvent of crystallization

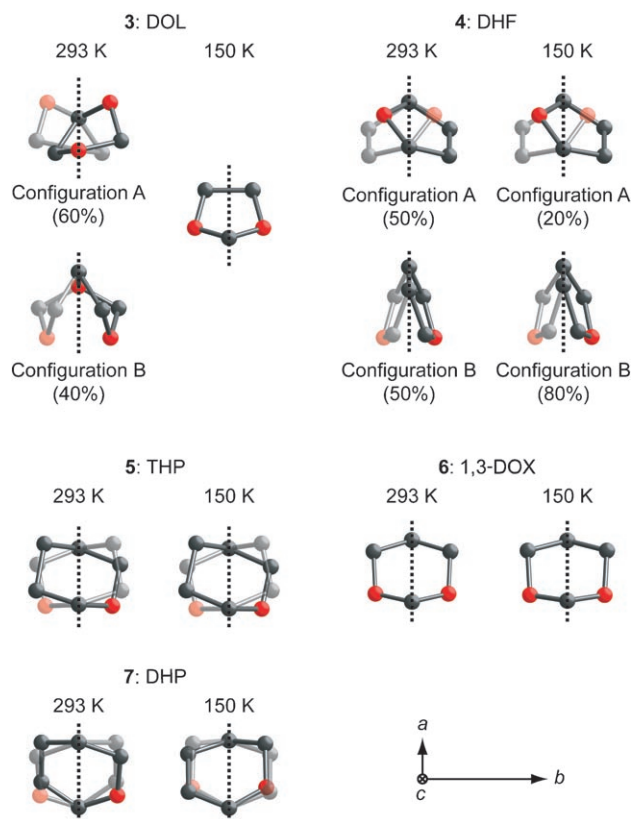


Figure 5. Molecular structures of the solvent of crystallization viewed along the crystallographic *c* axis. Dotted lines indicate mirror planes parallel to the *ac* plane.

is also observed in **4** and the ratio of configurations A and B is 50:50. The existence of the two configurations for the solvent of crystallization in salts **2–4** seems to be related to the size of the five-membered cyclic molecules, which are smaller than the cavities formed by the $[\text{Au}(\text{CN})_4]^-$ ion. On the other hand, the mode of disorder is simpler for the salts including six-membered cyclic molecules. The disorder of the solvent of crystallization in salts **5** and **7** is based on only one asymmetric unit, and only positional disorder induced by the mirror symmetry operation is observed. Furthermore, the 1,3-DOX molecule in salt **6** shows ordered configuration at 293 K and it is consistent with the mirror symmetry of the 1,3-DOX molecule itself. The five-membered cyclic molecule DOL also has mirror symmetry, and the ordered configuration is observed at 150 K.

The DHF and THP molecules have mirror symmetry, as do the 1,3-DOX and DOL molecules, but the disorder of the DHF and THP molecules still remains at 150 K. The ratio of configurations A and B of the DHF molecule is 20:80, and positional disorder induced by the mirror symmetry operation is inevitable for both DHF and THP. To achieve

the ordered configuration for DHF and THP, the mirror planes of the molecules must be congruent with the mirror plane of the crystal; at least the oxygen atom must lie in the mirror plane. However, such an arrangement is disadvantageous in view of the larger steric repulsion of the hydrogen atoms between the solvent of crystallization and donor molecules along the crystallographic *b* axis compared with formation of $\text{CH}\cdots\text{O}$ hydrogen bonds.

Temperature-dependent resistivity of salts **2–7**, measured perpendicular to the conducting *ac* plane, are shown in Figure 6. Broad maxima around 100 K, which resemble those of the κ -type BEDT-TTF salts,^[11,17] were observed except for salt **3**, and a distinct resistivity drop at the superconducting transition was observed at $T_c(\text{onset}) = 3.0$ K for **2**, 4.2 K for **4**, 4.5 K for **5**, 2.6 K for **6**, and 5.3 K for **7**. Although a resistivity drop of salt **3**, which seems to indicate superconducting transition, was also observed at 1.7 K for several crystals with reliable reproducibility, complete superconductivity of **3** has not been confirmed due to its low transition temperature and the cooling limit of the measurement apparatus. It is well known that the broad maximum of resistivity in the high-temperature range and the superconducting transition of the κ -type salts are simultaneously suppressed under applied pressure.^[11,18] The DOL molecule is the smallest among the solvents of crystallization of the six κ_L salts, and no resistivity maximum was observed for **3**. Therefore, the effect of chemical pressure may be intrinsic to **3**, and the superconducting transition is suppressed below 2 K. Superconductivity of **2**, **4**, **5**, **6**, and **7** was also confirmed by magnetic susceptibility measurements (Figure 7). The onset temperatures of the diamagnetic transitions are 2.8 K for **2**, 4.0 K for **4**, 4.5 K for **5**, 2.5 K for **6**, and 5.0 K for **7**, respectively. The volume fraction of superconductivity at 1.9 K is about 25, 80, 30, 10, and 20% of the perfect diamagnetism for **2**, **4**, **5**, **6**, and **7**, respectively, and all these salts are bulk organic superconductors.

The relationship between the cell volume at 293 K and T_c (onset) for salts **2–7** is shown in Figure 8. The T_c for salt **2** is lower than that of salt **5**, and the structural difference between **2** and **5** is the ring size of the solvent of crystallization. Salt **2** contains five-membered cyclic THF, whereas salt **5** contains six-membered cyclic THP. A similar relationship between T_c and the number of the ring atoms in the solvent of crystallization is observed between **3/6** and **4/7**, and it is consistent with the chemical-pressure effect caused by the size of the solvent of crystallization.

The T_c values for salts **2**, **3**, **5**, and **6** depend in a roughly linear fashion on cell volume, and those of salts **4** and **7** deviate from this linearity. These correlations suggest some additional effects on T_c of salts **4** and **7** apart from the ring size of the solvent of crystallization. The cell volumes of salts **4** and **7** are smaller than those of salts **2** and **5**, and this is consistent with the smaller size of the DHF and DHP molecules, which include a C=C double bond in the molecular skeleton. However, the *c* axis of salt **4** and the *a* axis of the salt **7** are longer than those of salts **2** and **5**, respectively (see Tables 2 and 3). The effect of the anisotropic changes in

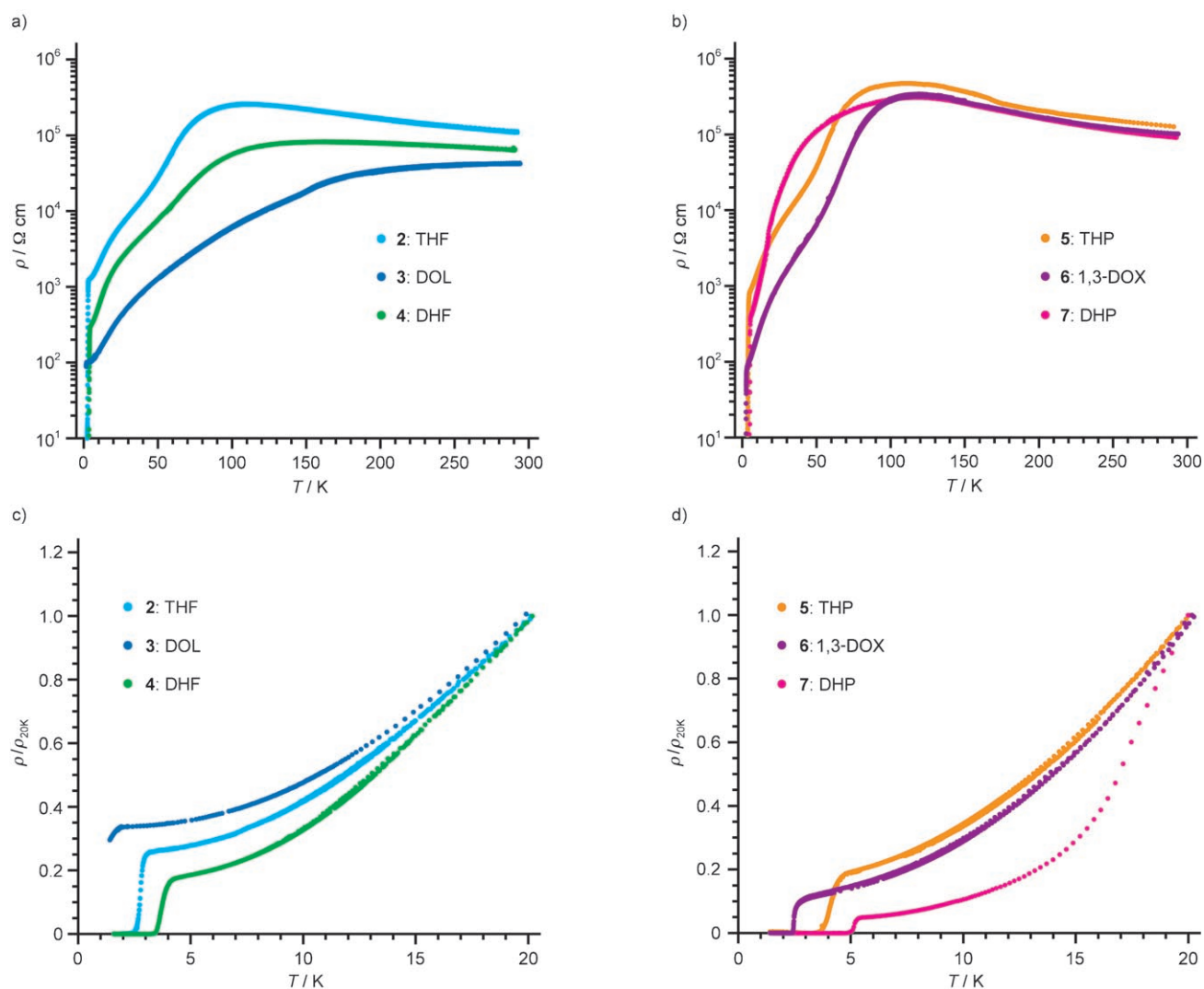


Figure 6. Temperature dependence of resistivity for a) 2–4 and b) 5–7, measured perpendicular to the conducting *ac* plane. c) and d) show temperature dependence of the normalized resistivity in the low-temperature region for 2–4 and 5–7, respectively.

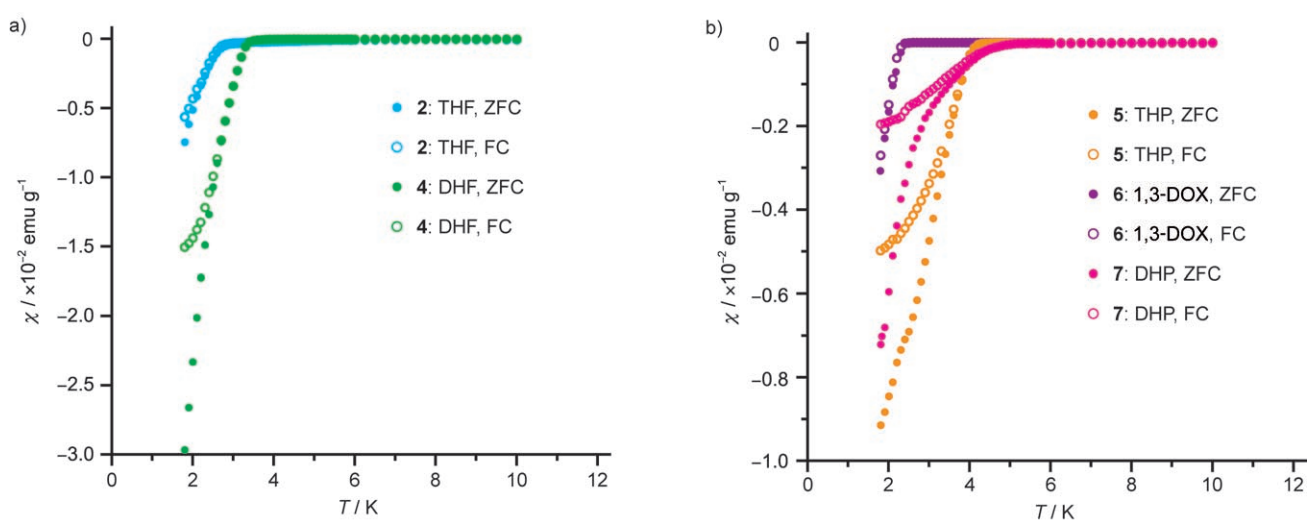


Figure 7. Temperature dependence of zero-field cooled (ZFC, closed circle) and field-cooled (FC, open circle) dc magnetization for a) 2, 4 and b) 5–7 in an applied field of 10 Oe.

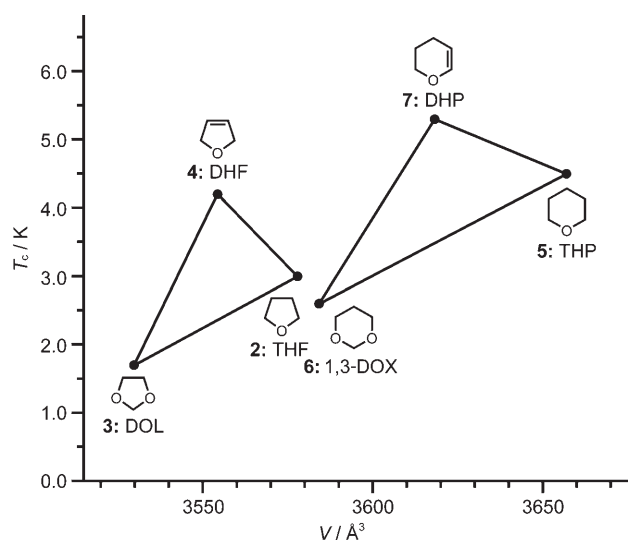


Figure 8. Relationship between cell volume $V[\text{Å}^3]$ at 293 K and the T_c (onset) [K] for **2–7**. The onset temperature of the resistivity drop for **3** is used as the T_c indicating superconductivity.

the shape of the solvent of crystallization, which corresponds to the anisotropic chemical-pressure effect for salts **4** and **7**, seems to be one of the origins of the deviation from the linear relationship between the T_c and cell volume. The effect of the anisotropic pressure on superconductivity of organic superconductors has already been reported for the uniaxial strain dependence of T_c of κ -type superconductors.^[19,20] For example, the increase in T_c for κ -(BEDT-TTF)₂Cu₂(CN)₃, in which the conducting donor layer is formed along the bc plane,^[21] was observed by applying uniaxial strain independently along the b and c axes.^[19]

Another interesting feature of the new series of organic superconductors is the thickness of the insulating layer (ca. 4.5–5.0 Å at 293 K),^[16] which completely separates the conducting donor layers. The transition temperatures of **2–7** are relatively high compared with those of the known κ -type superconductors based on unsymmetrical π donors,^[8e,22] and the characteristic CH \cdots N hydrogen bonds between the donor molecule and the counter anion likely play an important role in the superconductivity, because electron transport through the anion layer must occur to achieve bulk superconductivity. It has already been reported that weak donor \cdots anion interactions sometimes influence the physical properties in classical TMTSF and BEDT-TTF salts.^[23]

Intermolecular overlap integrals^[24] for the five new salts **3–7**, calculated on the basis of the structure at 293 and 150 K, are summarized in Table 5 together with those of salt **2** at 293 K. As in the known κ -type BEDT-TTF salts,^[25] intradimer overlap integrals $b1$ are considerably larger than the interdimer overlap integrals $b2$. The electronic band dispersions and Fermi surfaces of salts **2–7** were calculated within the tight-binding approximation by using these overlap integrals. Four bands are built from the HOMOs of the donor molecules in the conducting donor layer, and the upper and lower two bands, which are separated by a gap

Table 5. Calculated overlap integrals^[a] ($\times 10^{-3}$) for **2** on the basis of the structure at 293 K^[b] and **3–7** on the basis of the structure at 293 and 150 K.

Compound (solv.)	T [K]	$b1$	$b2$	p	q	$ b2/q $
2 (THF)	293	-20.63	-9.32	0.21	4.25	2.19
3 (DOL)	293	-20.32	-9.85	0.37	4.16	2.37
	150	-21.87	-10.47	0.75	4.32	2.42
4 (DHF)	293	-19.95	-9.80	0.09	4.15	2.36
	150	-21.75	-10.24	0.39	4.34	2.36
5 (THP)	293	-20.87	-9.22	0.30	3.94	2.34
	150	-23.31	-10.21	0.45	4.35	2.35
6 (1,3-DOX)	293	-21.73	-9.04	0.53	4.16	2.17
	150	-23.02	-9.33	1.00	4.08	2.29
7 (DHP)	293	-22.04	-8.81	0.67	4.24	2.08
	150	-23.75	-9.23	1.05	4.25	2.17

[a] See Figure 4a for definition of the overlap integrals. [b] From reference [12].

due to strong dimerization, are degenerate on the zone boundary (Figure 9a). As shown in Figure 9b, the calculated Fermi surfaces for the salts of κ_L -phases **2–7** are in the range from opened quasi-two-dimensional to closed two-dimensional. The overlap integrals $b2$ and q connect adjacent dimers along the a and c axes, respectively, and it has been reported that the degree of two-dimensionality can be estimated by the ratio of these two interdimer overlap integrals.^[25] Indeed, the $|b2/q|$ value of **7**, which shows the highest T_c , is the smallest (2.08 at 293 K) among the six κ_L salts and it suggests the strongest two-dimensional character. However, there is no general consistency between T_c and the dimensionality of the calculated Fermi surfaces throughout the six κ_L salts. To explain each contradiction between T_c and the dimensionality of the calculated Fermi surfaces, experimental information on the Fermi surfaces and optimization of the Hückel parameters of O and Se atoms for DMEDO-TSeF are required.^[26]

κ' -(DMEDO-TSeF)₂[Au(CN)₄](solv.): Two cation-radical salts of the κ' -phase containing DOL (**8**) or 1,4-DOX (**9**) as solvent of crystallization are isostructural and crystallize in the monoclinic space group Cc (Table 6). X-ray structure analyses were performed at 293 K for both salts and at 150 K for **9**. Low-temperature structure analysis for **8** was also performed repeatedly at 150 K, but the structure refinement for **8** did not converge because of crystal fragility, in spite of a slow cooling rate of less than 1 K min⁻¹.

The donor/anion/solvent ratios of **8** and **9** are 2:1:1, and the ratios and the species of the solvents of crystallization were confirmed by elemental analyses and ¹H NMR spectroscopy, respectively. The molecular arrangement of salt **9** at 293 K viewed along the crystallographic b axis is shown in Figure 10. There are two layers A and A' in the unit cell and they are crystallographically equivalent. As in the salts of the κ_L -phase, many CH \cdots N hydrogen bonds are formed between the donor molecule and the [Au(CN)₄]⁻ ion.

As shown in Figure 11a, the conducting donor layer consists of crystallographically independent donor molecules I and II, and the packing motif is of the so-called κ -type. Mol-

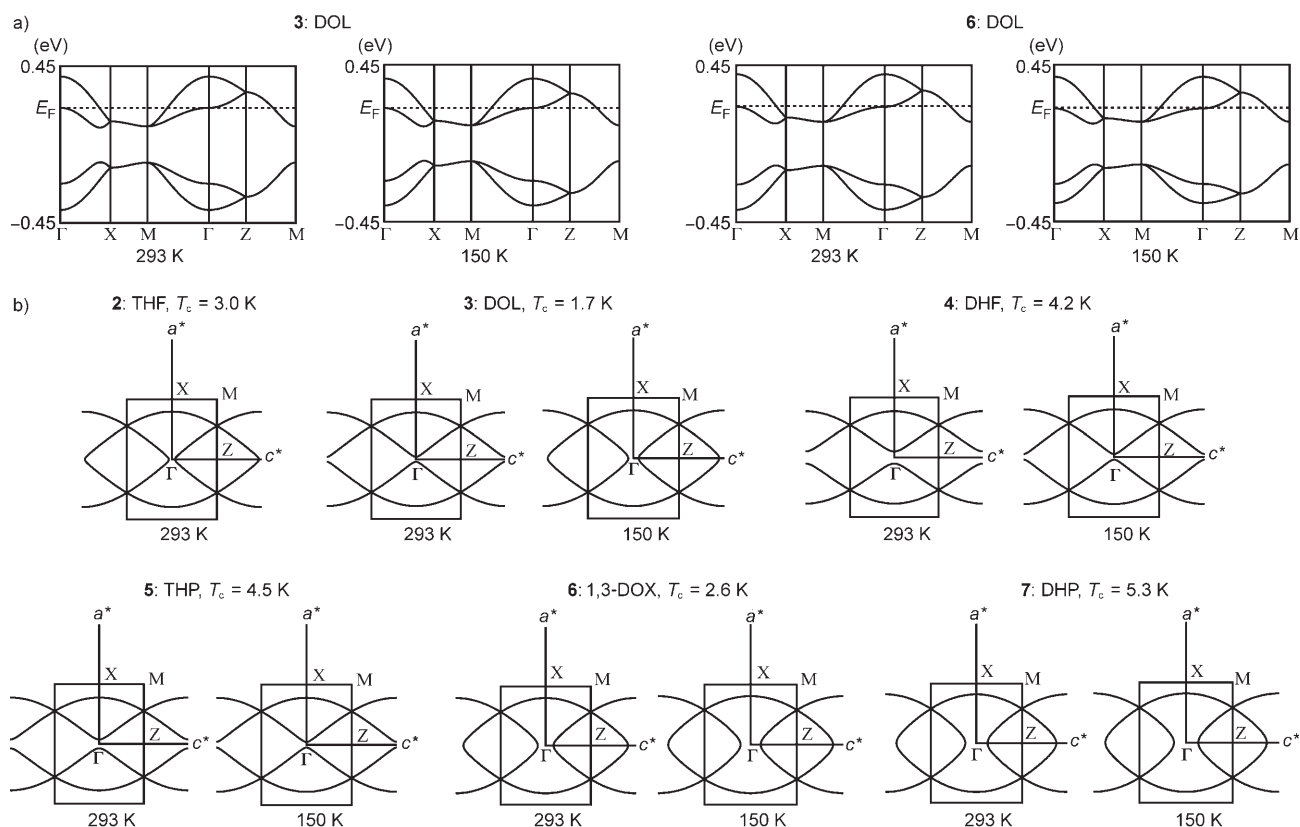


Figure 9. Calculated electronic band structures for κ_L salts at 293 and 150 K: a) Band dispersions of **3** and **6**. b) Fermi surfaces of **2–7**.

Table 6. Crystal data and transition temperature T_c (onset) for the κ' -phases **8** and **9**.

Compound (solv.)	8 (DOL)	9 (1,4-DOX)
T [K]	293	293
formula	$C_{27}H_{26}AuN_4O_6Se_8$	$C_{28}H_{28}AuN_4O_6Se_8$
formula weight	1331.16	1345.19
crystal system	monoclinic	monoclinic
space group	Cc (no. 9)	Cc (no. 9)
a [Å]	38.806(7)	38.954(7)
b [Å]	11.112(2)	11.2180(19)
c [Å]	8.2431(15)	8.2845(14)
β [°]	96.910(3)	97.206(3)
V [Å ³]	3528.6(11)	3591.6(11)
Z	4	4
ρ_{calcd} [g cm ⁻³]	2.506	2.488
μ [mm ⁻¹]	12.467	12.250
independent reflections	8806	8989
observed reflections [$I > 2\sigma(I)$]	6553	6962
variable parameters	433	442
R_{int}	0.0637	0.0793
GOF	0.960	0.910
$R1, wR2$ [$I > 2\sigma(I)$]	0.0425, 0.1014	0.0398, 0.0831
$R1, wR2$ (all data)	0.0577, 0.1045	0.0517, 0.0983
Flack parameter	0.062(11)	-0.027(10)
thickness of insulating layer [Å]	4.6	4.6
T_c [K]	— ^[a]	4.2

[a] Metallic down to 1.4 K.

ecules I and II form head-to-tail dimers, and a two-dimensional κ -type structure is constructed in the bc plane. The $CH\cdots O$ hydrogen bonds (dotted lines in the figure) are

formed between donor molecules I–I and II–II, and the network runs along the c axis. The $[Au(CN)_4]^-$ ions and the solvent of crystallization are located on $a \approx 0.15$ and form thick

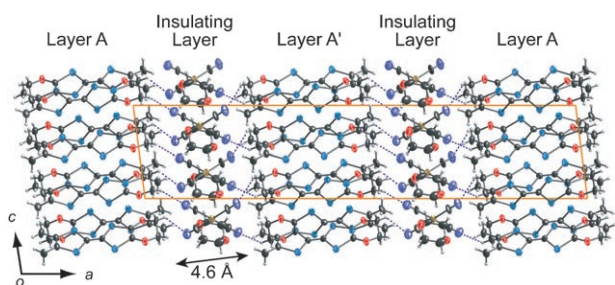


Figure 10. Molecular packing motif for **9** at 293 K. Dotted lines indicate CH...N contacts shorter than 2.75 Å. The minor orientations of the disordered ethylene bridge of the donor molecule are omitted for clarity.

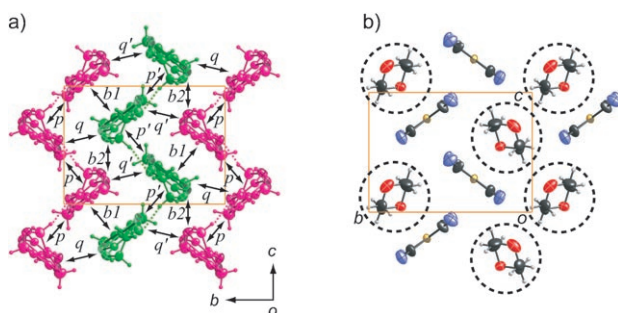


Figure 11. a) Donor arrangement of **9** at 293 K viewed along the crystallographic *a* axis with molecules I and II represented in red and green, respectively. Dotted lines indicate CH...O contacts shorter than 2.72 Å. The minor orientations of the disordered ethylene bridge of the donor molecule are omitted for clarity. b) Crystal structure of the insulating layer for **9** at 293 K, projected onto the *bc* plane.

insulating layers (ca. 4.5–4.6 Å, see Table 6). The solvent of crystallization molecules, DOL in **8** and 1,4-DOX in **9**, show an ordered structure and are located in cavities formed by the herringbone-type arrangement of anions (Figure 11 b).

The ethylene bridges of molecules I and II show disorder due to flipping (Figure 12), and distributions of the major and minor orientations are summarized in Table 7. The ethylene bridge of donor molecule II shows an ordered conformation at 150 K, whereas the disorder of the ethylene bridge of the molecule I remains at 150 K.

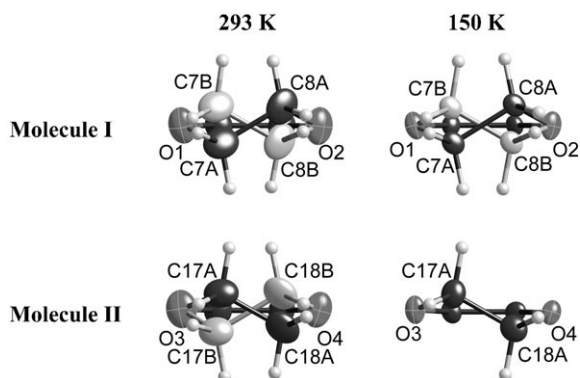


Figure 12. Conformations of the ethylenedioxy group of the crystallographically independent DMEDO-TSeF molecules I and II for **9** at 293 K and 150 K. The gray atoms and bonds represent the minor orientations of the disordered ethylene bridge.

Table 7. Distributions of two orientations of the ethylene bridges.

Compound (solv.)	<i>T</i> [K]		Major [%]	Minor [%]
8 (DOL)	293	molecule I	59(2)	41(2)
		molecule II	67(2)	33(2)
9 (1,4-DOX)	293	molecule I	67(2)	33(2)
		molecule II	74(2)	26(2)
	150	molecule I	71(1)	29(1)
		molecule II	100	0

Temperature dependences of the resistivity for **8** and **9** measured perpendicular to the conducting *bc* plane are shown in Figure 13. A broad maximum of the resistivity

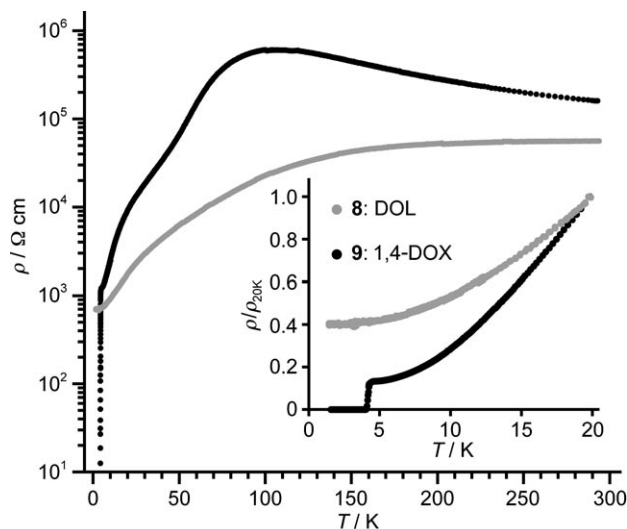


Figure 13. Temperature dependence of resistivity for **8** and **9** measured perpendicular to the conducting *bc* plane. The inset shows the normalized resistivity in the low-temperature region.

around 100 K was observed in salt **9**, and a superconducting transition occurred at $T_c(\text{onset})=4.2$ K. On the other hand, the resistivity of salt **8** monotonously decreases with lowering temperature, and a superconducting transition was not detected down to 1.4 K. The difference in conducting behavior between **8** and **9** is explained by the chemical-pressure effect, as for the κ_L -phase. The superconductivity of **9** was also confirmed by magnetic susceptibility measurements (Figure 14). The onset temperature of the diamagnetic transition is 4.2 K, which is the same as $T_c(\text{onset})$ in the resistivity measurements. The calculated volume fraction of superconductivity at 1.9 K is about 60% of the perfect diamagnetism, that is, **9** is also a bulk organic superconductor. Most organic superconductors have an inversion center in their crystal, and salt **9**, which has no inversion center, is the second noncentrosymmetric organic superconductor based on unsymmetrical π donors after (DTEDT)₃[Au(CN)₂].^[27]

The calculated overlap integrals on the basis of the structure at 293 K for both salts and at 150 K for **9** are listed in Table 8. In both salts, the intradimer overlap integrals *b1* are much larger than the interdimer overlap integrals *b2*, *p*, *p'*, *q*, and *q'*. Four bands are built from the HOMOs of the four donor molecules in the primitive cell ($a_p=(a-b)/2$, $b_p=b$,

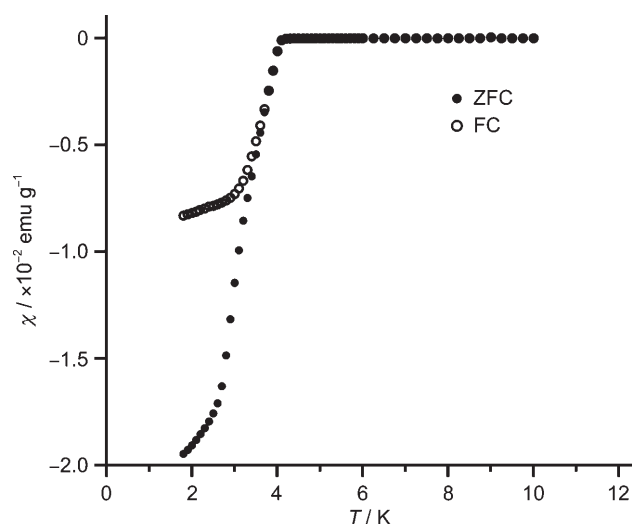


Figure 14. Temperature dependence of ZFC (closed circle) and FC (open circle) DC magnetizations for **9** in an applied field of 10 Oe.

$c_p=c$), and they resemble those of the κ_L -phase salts except for the energy gap on the zone boundary (Figure 15a). As shown in Figure 15b, the calculated Fermi surfaces of salt **9** at 293 and 150 K are opened and those of **8** at 293 K are almost the same.

Table 8. Calculated overlap integrals^[a] ($\times 10^{-3}$) for **8** on the basis of the structure at 293 K and for **9** on the basis of the structure at 293 and 150 K.

Compound (solv.)	T [K]	b1	b2	p	p'	q	q'
8 (DOL)	293	-20.93	-10.04	0.28	-0.36	3.86	4.91
9 (1,4-DOX)	293	-19.87	-9.57	0.28	-0.61	3.58	4.48
	150	-21.15	-10.30	0.50	-0.52	3.57	4.72

[a] See Figure 11 a for definition of the overlap integrals.

Conclusion

In addition to κ_H - and κ_L -(DMEDO-TSeF)₂[Au(CN)₄](THF) (**1**: κ_H -phase; **2**: κ_L -phase), seven cation radical salts (**3–9**) have now joined the family of three-component organic metals κ -(DMEDO-TSeF)₂[Au(CN)₄](solv.) (solv.=cyclic ether), and eight of them show superconductivity at ambient pressure. The number of superconducting salts derived from DMEDO-TSeF is the same as that of DMET, which is the first and the largest source of organic superconductors based on unsymmetrical π donors.^[8] The T_c values of the organic superconductors based on DMEDO-TSeF (1.7–5.3 K) are much higher than those of DMET (0.55–1.9 K), and they show superconductivity at ambient pressure. One of the origins of the superiority of the DMEDO-TSeF salts with regard to superconductivity is derived from the sulfur-free skeleton of the donor molecule, that is, the inner TSeF skeleton extends the electronic dimensionality and the small ethylenedioxy group instead of the ethylenedithio group may apply chemical pressure in the crystal.

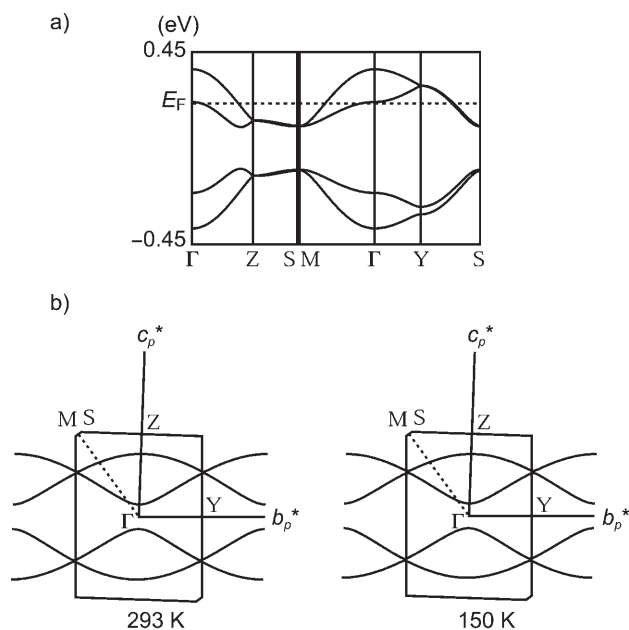


Figure 15. Calculated electronic band structures for κ' -salt **9**. a) Band dispersions at 293 K. b) Fermi surfaces at 293 (left) and 150 K (right).

The packing motifs of the κ -(DMEDO-TSeF)₂[Au(CN)₄](solv.) system have the so-called κ -type arrangement and they are further classified into κ_H -, κ_L -, and κ' -subphases according to differences in space-group symmetry. In the known κ -(BEDT-TTF)₂M(CF₃)₄(1,1,2-trihaloethane) system,^[11] three subphases (κ_H , κ_L and κ_L') have been reported, as in the present DMEDO-TSeF salts, but the crystal structure of the κ_H -phase could not be determined, and superconductivity of the κ_L' -phase has not been confirmed.^[11] On the other hand, the crystal structures of three subphases of the present system have been fully resolved, and distinct differences in superconductivity have been studied for all three subphases. The crystal structures of the DMEDO-TSeF salts are supported by CH \cdots O and CH \cdots N hydrogen bonds among the donor molecules and the counter anions, and they are in contrast to the complicated crystal structures of superconductors based on the parent BO molecule.^[3b,c] Recently, unconventional critical behavior was also reported for κ -type salts of BEDT-TTF,^[28] and the present κ -type superconductors based on the new π donor DMEDO-TSeF suggest extending the materials map of the unique phenomena of the κ -type salts.

The most interesting feature of the present new series of organic superconductors is dependence of the transition temperature of superconductivity on the solvent of crystallization. Among the six κ_L -type salts, the onset temperatures of the superconductivity are sensitive to the size and shape of the solvent of crystallization, as well as to the presence of a C=C double bond. A size effect of the solvent of crystallization on superconductivity has been reported for the above-mentioned BEDT-TTF system,^[11e] but the effect of shape, especially the anisotropic effect derived from the presence of a C=C double bond in the solvent of crystalliza-

tion, is predominant in this family. On the other hand, the appearance of the κ_{H} - and κ' -phases enables us to determine the structural limit of the solvent of crystallization for which the isomorphous crystal structure of the present system is maintained. This information on the relationship between superconductivity and molecular structure of the solvent of crystallization is interesting from the viewpoint of developing new organic superconductors. The design of new organic superconductors from scratch is extremely difficult, but tuning of T_{c} on the basis of modifying the solvent of crystallization is in progress, and accumulation of this knowledge will open the way to a new benchmark in organic superconductors.

Experimental Section

General: All chemicals and solvents were of reagent grade. All reactions were conducted under an argon atmosphere. Hexamethylphosphoric triamide (HMPT) was purchased from Sigma-Aldrich Japan K.K. and used without further purification. Column chromatography was carried out with silica gel (Kanto Chemical Co., Inc., 100–210 μm). Preparative gel-permeation chromatography (GPC) was performed on Japan Analytical Industry Co., Ltd. LC-908W equipped with JAI-GEL 1H, 2H column assembly. ^1H and ^{13}C NMR spectra were recorded on a JEOL JNM-Alpha400 spectrometer operating at 400 MHz for ^1H and 100 MHz for ^{13}C . The chemical shifts are reported downfield from internal Me_4Si . Mass spectra were recorded in EI mode with an ionization energy of 70 eV on a Shimadzu QP-5050A quadrupole mass spectrometer. The melting points were determined from the TG-DTA analyses on an SII EXSTAR6000 analyzer. IR spectra were recorded on a Shimadzu FTIR-8100M spectrometer with a PIKE MIRacle diamond ATR. Elemental analyses were performed at the Advanced Development & Supporting Center, RIKEN.

Dimethyl(ethylenedioxy)tetraselenafulvalene (DMEDO-TSeF): HMPT (0.74 mL, 4.1 mmol) was added to a mixture of selone **10**^[5a] (226 mg, 0.68 mmol) and selone **11**^[29] (215 mg, 0.71 mmol) in benzene (90 mL) at room temperature, and the solution was stirred for 2 h. After the removal of the solvent under reduced pressure, the crude products were separated by column chromatography ($\text{SiO}_2/\text{CS}_2\text{--CH}_2\text{Cl}_2$) and then purified by preparative GPC (CS_2). The target DMEDO-TSeF was isolated as purple-red needles (31 mg, 0.065 mmol, 10%). M.p. 199 °C (decomp); ^1H NMR (400 MHz, CD_2Cl_2): δ = 4.27 (s, 4H; $\text{OCH}_2\text{CH}_2\text{O}$), 2.00 ppm (s, 6H; CH_3); ^{13}C NMR (100 MHz, CD_2Cl_2): δ = 127.33, 125.85, 109.38, 93.04, 67.03, 16.28 ppm; IR (neat): $\tilde{\nu}$ = 1624 (s), 1443 (m), 1368 (m), 1268 (m), 1240 (w), 1134 cm^{-1} (s); MS (70 eV, EI): m/z : 480 [M^+ for $\text{C}_{10}\text{H}_{10}\text{O}_2\text{Se}^{80}\text{Se}_3$]; elemental analysis calcd (%) for $\text{C}_{10}\text{H}_{10}\text{O}_2\text{Se}_4$: C 25.13, H 2.11; found: C 25.14, H 2.11.

Cyclic voltammetry: The cyclic voltammogram of DMEDO-TSeF was recorded on a BAS ALS-model 610A analyzer in a benzonitrile solution of Bu_4NBF_4 (0.1 M), and glassy carbon working and Pt auxiliary electrodes were employed. The sweep rate was 100 mV s^{-1} . Potentials were referenced to Ag/AgNO_3 standard electrode and were calibrated versus the $\text{Cp}_2\text{Fe}/\text{Cp}_2\text{Fe}^+$ couple recorded under the same conditions.

Crystal preparation: Single crystals of the $[\text{Au}(\text{CN})_4]^-$ salts of DMEDO-TSeF were prepared by galvanostatic oxidation under the conditions listed in the Supporting Information. THF and 1,4-DOX were purchased from Kanto Chemical Co., Inc. and used without further purification. THP and dichloromethane were purchased from Sigma-Aldrich Japan K.K. and Dojindo Laboratories and used without further purification. DHF, DOL, DHP, and 1,3-DOX were purchased from Tokyo Chemical Industry Co., Ltd. and distilled before use. Cyclohexane was purchased from Junsei Chemical Co., Ltd. and distilled before use. Platinum wire electrodes (1.0 mm \varnothing) and standard H-shaped cells were employed. The identity of the solvent of crystallization was confirmed by ^1H NMR spec-

troscopy on a sonicated suspension containing dried crystals of each salt, and the donor/anion/solvent ratios of the salts were determined by elemental analysis as follows:

Mixture of 3 and 8 (DOL): elemental analysis calcd (%) for $\text{C}_{27}\text{H}_{26}\text{AuN}_4\text{O}_6\text{Se}_8$: C 24.36, H 1.97, N 4.21; found: C 24.07, H 1.90, N 4.19.

4 (DHF): elemental analysis calcd (%) for $\text{C}_{28}\text{H}_{26}\text{AuN}_4\text{O}_5\text{Se}_8$: C 25.34, H 1.97, N 4.22; found: C 25.20, H 1.95, N 4.18.

5 (THP): elemental analysis calcd (%) for $\text{C}_{29}\text{H}_{30}\text{AuN}_4\text{O}_5\text{Se}_8$: C 25.93, H 2.25, N 4.17; found: C 25.74, H 2.26, N 4.17.

6 (1,3-DOX): elemental analysis calcd (%) for $\text{C}_{28}\text{H}_{28}\text{AuN}_4\text{O}_6\text{Se}_8$: C 25.00, H 2.10, N 4.17; found: C 24.87, H 2.04, N 4.13.

7 (DHP): elemental analysis calcd (%) for $\text{C}_{29}\text{H}_{28}\text{AuN}_4\text{O}_5\text{Se}_8$: C 25.97, H 2.10, N 4.18; found: C 25.63, H 2.14, N 4.19.

9 (1,4-DOX): elemental analysis calcd (%) for $\text{C}_{28}\text{H}_{28}\text{AuN}_4\text{O}_6\text{Se}_8$: C 25.00, H 2.10, N 4.17; found: C 24.95, H 2.04, N 4.14.

X-ray crystallographic analysis: Diffraction data were collected on a Bruker AXS SMART-APEX CCD system with graphite-monochromatized $\text{MoK}\alpha$ radiation ($\lambda = 0.71073 \text{ \AA}$). Raw frame data were integrated using SAINT,^[30] face-indexed absorption corrections^[31] were applied for the cation-radical salts **3–9**, and empirical absorption corrections using SADABS^[32] were applied for neutral DMEDO-TSeF. The structures were solved by the direct method (SHELXS-97^[33]) and refined by full-matrix least-squares techniques on F^2 (SHELXTL).^[34] CCDC-637835 (DMEDO-TSeF at 293 K), CCDC-637836 (DMEDO-TSeF at 150 K), CCDC-637837 (**3** at 293 K), CCDC-637838 (**3** at 150 K), CCDC-637839 (**4** at 293 K), CCDC-637840 (**4** at 150 K), CCDC-637841 (**5** at 293 K), CCDC-637842 (**5** at 150 K), CCDC-637843 (**6** at 293 K), CCDC-637844 (**6** at 150 K), CCDC-637845 (**7** at 293 K), CCDC-637846 (**7** at 150 K), CCDC-637847 (**8**), CCDC-637848 (**9** at 293 K), and CCDC-637849 (**9** at 150 K) contain the supplementary crystallographic data for this paper. These data can be obtained free of charge from the Cambridge Crystallographic Data Centre via www.ccdc.cam.ac.uk/data_request/cif.

Electronic band calculations: Intermolecular overlap integrals were calculated by using the HOMOs of the donor molecules obtained by extended Hückel MO calculations with the semiempirical parameters for the s and p Slater-type atomic orbitals listed in the Supporting Information. The electronic band dispersions and Fermi surfaces were calculated by using the intermolecular overlap integrals under the tight-binding approximation.^[24]

Electrical resistivity: The dc electrical resistivities were measured by the standard four-probe method in the temperature range of 1.4–300 K. Gold wires (10 or 18 μm) were attached to a single crystal by using carbon paste, and silver paste was used to connect the gold wires to the measurement substrate.

Magnetic susceptibility: Magnetic susceptibilities were measured on a Quantum Design SQUID magnetometer (MPMS-XL5) for randomly oriented samples in the temperature range of 1.9–10 K with a dc magnetic field of 10 Oe. The diamagnetism of the sample holder was obtained from blank experiments under the same conditions as those for the sample measurements. The diamagnetic core susceptibilities of the DMEDO-TSeF molecule, $[\text{Au}(\text{CN})_4]^-$ anion and solvent of crystallization were evaluated with Pascal's table: χ_{dia} [emu mol^{-1}]: DMEDO-TSeF -1.74×10^{-4} ; $[\text{Au}(\text{CN})_4]^-$ -1.04×10^{-4} ; THF -0.53×10^{-4} ; DOL -0.42×10^{-4} ; DHF -0.65×10^{-4} ; THP -0.46×10^{-4} ; 1,3-DOX -0.58×10^{-4} ; DHP -0.54×10^{-4} ; 1,4-DOX -0.58×10^{-4} .

Acknowledgement

We thank Dr. Kenji Yoza (Bruker AXS K.K.) for his kind advice on crystal structure analysis.

- [1] H. Yamochi in *TTF Chemistry—Fundamentals and Applications of Tetrathiafulvalene: Oxygen Analogues of TTFs* (Eds.: J. Yamada, T. Sugimoto), Kodansha & Springer, Tokyo, **2004**, Chap. 4, pp. 83–118.
- [2] T. Suzuki, H. Yamochi, G. Srdanov, K. Hinkelmann, F. Wudl, *J. Am. Chem. Soc.* **1989**, *111*, 3108–3109.
- [3] a) S. Horiuchi, H. Yamochi, G. Saito, K. Sakaguchi, M. Kusunoki, *J. Am. Chem. Soc.* **1996**, *118*, 8604–8622; b) M. A. Beno, H. H. Wang, A. M. Kini, K. D. Carlson, U. Geiser, W.-K. Kwok, J. E. Thompson, J. M. Williams, J. Ren, M.-H. Whangbo, *Inorg. Chem.* **1990**, *29*, 1599–1601; c) S. Kahlich, D. Schweitzer, I. Heinen, S. E. Lan, B. Nuber, H. J. Keller, K. Winzer, H. W. Helberg, *Solid State Commun.* **1991**, *80*, 191–195.
- [4] M. Chollet, L. Guerin, N. Uchida, S. Fukaya, H. Shimoda, T. Ishikawa, K. Matsuda, T. Hasegawa, A. Ota, H. Yamochi, G. Saito, R. Tazaki, S. Adachi, S. Koshihara, *Science* **2005**, *307*, 86–89.
- [5] a) T. Imakubo, T. Shirahata, M. Kibune, *Chem. Commun.* **2004**, 1590–1591; b) T. Imakubo, M. Kibune, T. Shirahata, *Mol. Cryst. Liq. Cryst.* **2006**, *455*, 65–70.
- [6] T. Shirahata, M. Kibune, T. Imakubo, *J. Mater. Chem.* **2005**, *15*, 4399–4402.
- [7] K. Bechgaard, D. O. Cowan, A. N. Bloch, *J. Chem. Soc. Chem. Commun.* **1974**, 937–938.
- [8] a) K. Kikuchi, T. Namiki, I. Ikemoto, K. Kobayashi, *J. Chem. Soc. Chem. Commun.* **1986**, 1472–1473; b) K. Kikuchi, M. Kikuchi, T. Namiki, K. Saito, I. Ikemoto, K. Murata, T. Ishiguro, K. Kobayashi, *Chem. Lett.* **1987**, 931–932; c) K. Kikuchi, K. Murata, Y. Honda, T. Namiki, K. Saito, K. Kobayashi, T. Ishiguro, I. Ikemoto, *J. Phys. Soc. Jpn.* **1987**, *56*, 3436–3439; d) K. Kikuchi, K. Murata, Y. Honda, T. Namiki, K. Saito, H. Anzai, K. Kobayashi, T. Ishiguro, I. Ikemoto, *J. Phys. Soc. Jpn.* **1987**, *56*, 4241–4244; e) K. Kikuchi, Y. Honda, Y. Ishikawa, K. Saito, I. Ikemoto, K. Murata, H. Anzai, T. Ishiguro, K. Kobayashi, *Solid State Commun.* **1988**, *66*, 405–408.
- [9] D. Jerome, A. Mazaud, M. Ribault, K. Bechgaard, *J. Phys. Lett.* **1980**, *41*, L95–L98.
- [10] T. Imakubo, N. Tajima, M. Tamura, R. Kato, Y. Nishio, K. Kajita, *J. Mater. Chem.* **2002**, *12*, 159–161.
- [11] a) J. A. Schlueter, U. Geiser, J. M. Williams, H. H. Wang, W.-K. Kwok, J. A. Fendrich, K. D. Carlson, C. A. Achenbach, J. D. Dudek, D. Naumann, T. Roy, J. E. Schirber, W. R. Bayless, *J. Chem. Soc. Chem. Commun.* **1994**, 1599–1600; b) J. A. Schlueter, K. D. Carlson, U. Geiser, H. H. Wang, J. M. Williams, W.-K. Kwok, J. A. Fendrich, U. Welp, P. M. Keane, J. D. Dudek, A. S. Komosa, D. Naumann, T. Roy, J. E. Schirber, W. R. Bayless, B. Dodrill, *Physica C* **1994**, *233*, 379–386; c) J. A. Schlueter, J. M. Williams, U. Geiser, J. D. Dudek, S. A. Sirchio, M. E. Kelly, J. S. Gregar, W.-H. Kwok, J. A. Fendrich, J. E. Schirber, W. R. Bayless, D. Naumann, T. Roy, *J. Chem. Soc. Chem. Commun.* **1995**, 1311–1312; d) U. Geiser, J. A. Schlueter, J. M. Williams, A. M. Kini, J. D. Dudek, M. E. Kelly, D. Naumann, T. Roy, *Synth. Met.* **1997**, *85*, 1465–1466; e) J. A. Schlueter, J. M. Williams, U. Geiser, J. D. Dudek, M. E. Kelly, S. A. Sirchio, K. D. Carlson, D. D. Naumann, T. Roy, C. F. Campana, *Adv. Mater.* **1995**, *7*, 634–639; f) J. A. Schlueter, U. Geiser, A. M. Kini, H. H. Wang, J. M. Williams, D. Naumann, T. Roy, B. Hoge, R. Eujen, *Coord. Chem. Rev.* **1999**, *190*, 781–810; g) U. Geiser, J. A. Schlueter, *Chem. Rev.* **2004**, *104*, 5203–5241.
- [12] T. Shirahata, M. Kibune, T. Imakubo, *Chem. Commun.* **2006**, 1592–1594.
- [13] Takimiya et al. reported “partial” superconductivity for the Br salt of sulfur-free donor MDSe-TSF (methylenediselenotetraselenafulvalene) with a T_c of 4 K, but the diamagnetic shielding effect at 1.8 K for the Br salt is only 1% of that expected for a bulk superconductor, and no drop in resistivity was reported: M. Kodani, A. Takamori, K. Takimiya, Y. Aso, T. Otsubo, *J. Solid State Chem.* **2002**, *168*, 582–598.
- [14] T. Ishiguro, K. Yamaji, G. Saito, *Organic Superconductors*, 2nd ed., Springer, Berlin, **1998**.
- [15] A. Bondi, *J. Phys. Chem.* **1964**, *68*, 441–451.
- [16] The thickness of the insulating layer is based on the distance between the hydrogen edges of donor molecules; a distance of 4.4 Å is estimated for κ_1 -(BEDT-TTF)₂[Cu(CF₃)₄](1,1,2-trichloroethane)^[11a] using the same procedure.
- [17] a) H. Urayama, H. Yamochi, G. Saito, K. Nozawa, T. Sugano, M. Kinoshita, S. Saito, K. Oshima, A. Kawamoto, J. Tanaka, *Chem. Lett.* **1988**, 55–58; b) A. M. Kini, U. Geiser, H. H. Wang, K. D. Carlson, J. M. Williams, W.-K. Kwok, K. G. Vandervoort, J. E. Thompson, D. L. Stupka, D. Jung, M.-H. Whangbo, *Inorg. Chem.* **1990**, *29*, 2555–2557.
- [18] a) J. E. Schirber, E. L. Venturini, A. M. Kini, H. H. Wang, J. R. Whitworth, J. M. Williams, *Physica C* **1988**, *152*, 157–158; b) K. Murata, M. Tokumoto, H. Anzai, Y. Honda, N. Kinoshita, T. Ishiguro, N. Toyota, T. Sasaki, Y. Muto, *Synth. Met.* **1988**, *27*, A263–A270; c) I. D. Parker, R. H. Friend, M. Kurmoo, P. Day, C. Lenoir, P. Batail, *J. Phys. Condens. Matter* **1989**, *1*, 4479–4484; d) J. M. Williams, A. M. Kini, H. H. Wang, K. D. Carlson, U. Geiser, L. K. Montgomery, G. J. Pyrka, D. M. Watkins, J. M. Kommers, S. J. Boryschuk, A. V. S. Crouch, W.-K. Kwok, J. E. Schirber, D. L. Overmyer, D. Jung, M.-H. Whangbo, *Inorg. Chem.* **1990**, *29*, 3272–3274.
- [19] a) M. Maesato, Y. Shimizu, T. Ishikawa, G. Saito, *Synth. Met.* **2003**, *137*, 1243–1244; b) M. Maesato, Y. Shimizu, T. Ishikawa, G. Saito, K. Miyagawa, K. Kanoda, *J. Phys. IV* **2004**, *14*, 227–231; c) Y. Shimizu, M. Maesato, G. Saito, O. Drozdova, L. Ouahab, *Synth. Met.* **2003**, *133*, 225–226.
- [20] a) M. Tokumoto, T. Mizutani, T. Kinoshita, J. S. Brooks, Y. Uwatoko, O. Drozdova, K. Yakushi, I. Tamura, H. Kobayashi, T. Mangesu, J. Yamada, K. Ishida, *Mol. Cryst. Liq. Cryst.* **2002**, *380*, 227–235; b) T. Ishikawa, M. Maesato, G. Saito, *Synth. Met.* **2003**, *133*, 227–228; c) H. Ito, Y. Hasegawa, A. Ishihara, S. Takasaki, J. Yamada, H. Anzai, *Synth. Met.* **2003**, *133*, 233–234.
- [21] U. Geiser, H. H. Wang, K. D. Carlson, J. M. Williams, H. A. Charlier, Jr., J. E. Heindl, G. A. Yaconi, B. J. Love, M. W. Lathrop, J. E. Schirber, D. L. Overmyer, J. Ren, M.-H. Whangbo, *Inorg. Chem.* **1991**, *30*, 2586–2588.
- [22] a) G. C. Papavassiliou, G. A. Mousdis, J. S. Zambounis, A. Terzis, A. Hountas, B. Hilti, C. W. Mayer, J. Pfeiffer, *Synth. Met.* **1988**, *27*, B379–B383; b) J. S. Zambounis, C. W. Mayer, K. Hauenstein, B. Hilti, W. Hofherr, J. Pfeiffer, M. Bürkle, G. Rihs, *Adv. Mater.* **1992**, *4*, 33–35.
- [23] a) M. A. Beno, G. S. Blackman, P. C. W. Leung, J. M. Williams, *Solid State Commun.* **1983**, *48*, 99–103; b) J. M. Williams, M. A. Beno, H. H. Wang, P. C. W. Leung, T. J. Emge, U. Geiser, K. D. Carlson, *Acc. Chem. Res.* **1985**, *18*, 261–267.
- [24] T. Mori, A. Kobayashi, Y. Sasaki, H. Kobayashi, G. Saito, H. Inokuchi, *Bull. Chem. Soc. Jpn.* **1984**, *57*, 627–633.
- [25] T. Mori, *Bull. Chem. Soc. Jpn.* **1999**, *72*, 179–197.
- [26] For optimization of the Se Hückel parameter of the bis(ethylenedithio)tetraselenafulvalene (BETS) molecule, see: T. Mori, M. Katsuhara, *J. Phys. Soc. Jpn.* **2002**, *71*, 826–844.
- [27] Y. Misaki, N. Higuchi, H. Fujiwara, T. Yamabe, T. Mori, H. Mori, S. Tanaka, *Angew. Chem.* **1995**, *107*, 1340–1343; *Angew. Chem. Int. Ed. Engl.* **1995**, *34*, 1222–1225.
- [28] F. Kagawa, K. Miyagawa, K. Kanoda, *Nature* **2005**, *436*, 534–537.
- [29] K. Bechgaard, D. O. Cowan, A. N. Bloch, L. Henriksen, *J. Org. Chem.* **1975**, *40*, 746–749.
- [30] SAINT, Version 6.45, Bruker AXS, **2003**.
- [31] XPREP, Bruker AXS, **2003**.
- [32] SADABS: Program for Empirical Absorption Correction, G. M. Sheldrick, University of Göttingen, Göttingen, Germany, **1996**.
- [33] SHELXS97: Program for the Solution of Crystal Structures from X-ray Data, G. M. Sheldrick, University of Göttingen, Göttingen, Germany, **1997**.
- [34] SHELXTL Reference Manual, Version 5.03, Siemens Energy & Automation, Inc., Analytical Instrumentation: Madison, Wisconsin, USA, **1996**.

Received: February 26, 2007
Published online: July 3, 2007